Multi-Band UWB Sensor Networks for high density sub-surface diagnostic: Energy Consumption and Network Set-Up Delay *

I. L'Abbate
D.E.I., Politecnico di Milano
P.zza L. da Vinci, 32
I-20133 Milano, IT
CWC
P.O. Box 4500
FI-90014, Oulun Yliopsito, FI
isabella.labbate@mail.polimi.it
isalab@ee.oulu.it

S. Savazzi
D.E.I., Politecnico di Milano
P.zza L. da Vinci, 32
I-20133 Milano, IT
savazzi@elet.polimi.it

L. Goratti
CWC
P.O. Box 4500
FI-90014, Oulun Yliopsito, FI
goratti@ee.oulu.fi

U. Spagnolini
D.E.I., Politecnico di Milano
P.zza L. da Vinci, 32
I-20133 Milano, IT
spagnoli@elet.polimi.it

Matti Latva-aho
CWC
P.O. Box 4500
FI-90014, Oulun Yliopsito, FI
matti.latvaaho@ee.oulu.fi

ABSTRACT

Acquisition systems for sub-surface diagnostic (e.g., earthquake monitoring) require large number of sensors (geophones or accelerometers) to be deployed outdoor over large areas (tens of sqkm) to measure backscattered wave fields that are collected into a storage/processing unit (sink node). Aggregated data sets are analyzed to obtain an image of the sub-surface, monitor seismic activity, and declare possible alarm conditions. Cable based connectivity is the bottleneck of current systems, in terms of power consumption and degradation in accuracy. Replacing cables with wireless is now becoming attractive to improve the monitoring quality and reduce the probability of false negatives. Strict sampling synchronization constraint over large geographic areas, high precision sensor localization, high data-rate, and low delay are all topics that call for a scalable network system: Multi-Band Ultra Wide-Band radio transmissions (MB-UWB) play a key role as the only viable technology. This paper introduces the system and UWB network architecture based on ECMA-368 standard, moreover it provides a novel analytical tool to evaluate the energy consumption and delay during network set-up.

*This work is partially supported by Ministero dell' Istruzione dell' Università e della Ricerca MIUR-FIRB Integrated System for Emergency (InSyEme) project under the grant RBIP063BPH.

"IWCMC'10, June 28 - July 2, 2010, Caen, France.

Categories and Subject Descriptors

C.2 [**Computer-Communication Networks**]: Miscellaneous; B.4.4 [**Performance and Reliability**]: Performance Analysis and Design Aids

General Terms

Algorithms, Performance, Standardization

Keywords

Seismic monitoring, Multi Band OFDM, Ultra-Wide Band, Mesh networking, Distributed Beaconing

1. INTRODUCTION

Wireless Sensor Networks (WSNs) represent a well-known paradigm which collects a set of emerging technologies that will influence a range of industrial, scientific, and governmental applications. New radio technologies such as Ultra-Wide Band (UWB) and Multi-Band OFDM (MB-OFDM) [1] are expected to provide tiny and low power sensors capable to support raw data rates within very short range distances. These technologies can operate at low power without interfering with other wireless applications, therefore they are of interest for a wide class of heterogeneous networking systems (e.g., for monitoring and emergency management).

Seismic monitoring systems are used for sub-surface diagnostic to prevent and possibly predict small earthquakes, track under-ground movements, and propagate alarms. These systems typically require large number of sensors (geophones or accelerometers) to be deployed over wide areas to form large arrays that measure (and digitalize) back-scattered wave fields. A storage/processing unit (sink node) collects all the measurements from all the geophones/sensors, activate real-time telemetry in one or more areas of interest, and propagate alarms in case an emergency is declared. Acquisition systems can be classified into active and passive, de-

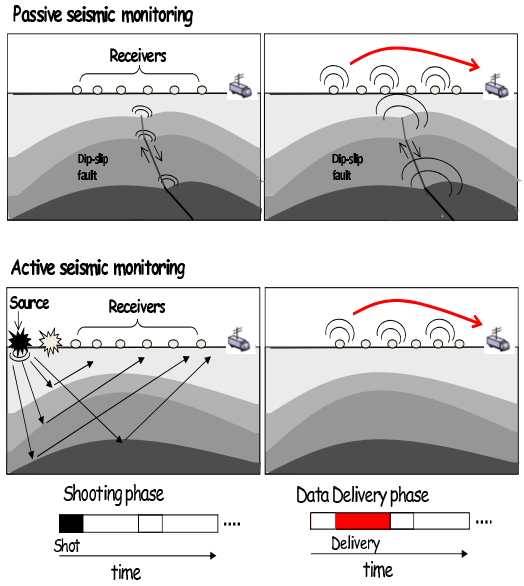

Figure 1: Example of seismic monitoring for sub-surface diagnostic: passive and active monitoring.

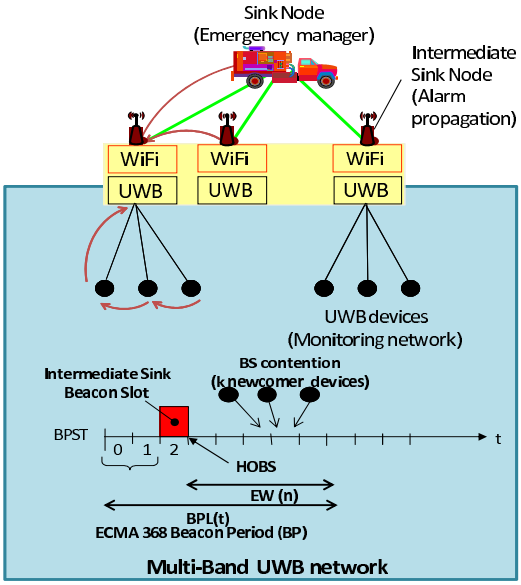

Figure 2: Network architecture for emergency monitoring and sub-surface diagnostic. MB-UWB sub-network and Beacon Period framing structure.

pending on the particular monitoring activity. As shown in Fig. 1, active monitoring systems (ASM) collect seismic data from all the sensors using seismic waves as probing signals (sources) to acquire a picture of the sub-surface, perform sub-surface diagnostic, and track underground movements. Passive monitoring systems (PSM) are instead designed to "listen" and analyze, in real-time, acoustic signals to identify earthquakes and perform on demand sub-surface diagnostic.

Cable based connectivity is the bottleneck of current systems. It causes large power consumption and degradation in accuracy. Switching from wired equipment to wireless geophones is now becoming attractive to improve the monitoring quality and reduce the probability of false negatives (fundamental in emergency management). In fact, geophones can be randomly deployed with higher densities customizing survey designs for specific sub-surface imaging objectives [7].

The large geographic areas to be typically monitored, the high precision sensor localization, the high data-rate (e.g., during active monitoring), and the low delay are all topics that call for a scalable heterogeneous wireless network system where MB-UWB radio transmissions play a key role along with other well consolidated technologies (e.g., WiFi).

This paper introduces in Sect. 2 the heterogeneous system architecture and the UWB network based on ECMA-368 standard [3]. Then in Sect. 3 it is provided a novel analytical tool for the evaluation of the energy consumption and delay during network set-up that can be used for the optimization of MAC layer parameters. Simulation results and (Sect. 4) provide an analysis of network performances by focusing on the random access delay and on the energy consumption, two key parameters for emergency management.

2. NETWORK ARCHITECTURE FOR SUB-SURFACE DIAGNOSTIC: MB-UWB

Since wireless network of geophones is required to monitor large extended fields, an heterogeneous network (long and short range radio technologies) appears as an attractive solution. As illustrated in Fig. 2, independent UWB sub-networks perform sub-surface diagnostic and monitor a limited region of space while propagating one or more possible alarm conditions to an intermediate access point (sink) for data aggregation. Intermediate sink (Fig. 2) might activate a long-range radio to connect with the remote storage unit (remote sink) and coordinate any necessary operation to manage an emergency situation.

UWB signals are confined in (unlicensed) frequency bands and with stringent emission power spectral density limitations so that they can be used for monitoring and for short-range transmissions in conjunction with other $2.4GHz$-based long-range radio technologies such as IEEE 802.11, without paying meaningful cross-interference [6]. The International Standard ECMA-368 [3] specifies the UWB physical layer (PHY) and the MAC for a high-speed, short-range wireless network. It defines the uses of 14 sub-bands above $3.1GHz$, each one of $528MHz$ [4]-[2], and prescribes the use of MB-OFDM to transmit data. MB-OFDM enables the transmission of extremely high-speed data (up to $480Mbps$) within short-ranges of up to $5-10$ meters and (expected) 30 meters in outdoor environments (data rates below $53Mbps$) [1].

2.1 ECMA-368 Distributed beaconing

In what follows the design of MB-UWB sub-networks is outlined, focusing on the so called distributed beaconing defined by ECMA-368 to manage the allocation of transmission resources in a completely distributed fashion. When an UWB device detects an emergency condition, it should activate the radio transceiver and acquire transmission resources. Since network density might be high, an efficient design (for delay and energy consumption) of the distributed beaconing during the network set-up is mandatory.

The channel time is divided into superframes (SF) of fixed duration, $65.536\ \mu s$. Each SF is divided in beacon period (BP), that implements the distributed beaconing, and data

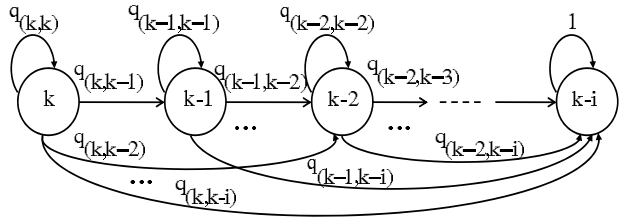

Figure 3: Absorbing MC or random walk.

transfer period (DTP). The BP is placed on top of the SF, it is divided in beacon slots (BS), and it is of finite size which can be up to mMaxBPLength BS [3]. The first two slots are referred to as signaling slots and are left for specific purposes. Before any other actions can take place, all UWB devices must acquire a unique BS following a S-Aloha like channel access. Since the BP is an interval of finite capacity, only a finite number of devices are allowed to join the network. ECMA-368 requires the maintenance of tight network synchronization, being the BP a slotted interval. The reference time for any device joining a particular group of devices is the beacon period start time (BPST) and it is issued by the active intermediate sink node (Fig. 2). When an UWB device activates the radio for opening the communication it must first scan for one SF to assess whether a BPST is present or not. If BPST is present, ECMA-368 defines the so called mechanism of extension and contraction to enable devices to acquire a unique BS in a distributed fashion. Unnecessary long BP yields to higher energy consumption: being UWB monitoring devices battery powered, energy efficient methods to manage the network (with low delay) are of fundamental importance.

During the extension phase (EP) the overall length of the BP, $BPL(t)$, is a function of time as newcomer devices might add asynchronously during different times (superframes). Similarly, the highest occupied busy slot (HOBS) varies with time according to the number of newcomer devices. The extension window (EW) is the number of empty slots left at the end of a BP to facilitate newcomer devices to join the network (see Fig. 2). ECMA-368 defines an EW of 8 slots, while it should be in principle optimally designed to be as short as possible. At a given SF, devices that attempt to acquire a BS make access on the EW and search for consensus. The consensus is achieved by comparing information carried in the beacon frames (beacon period occupancy information elements - BPOIE) propagated by devices that are already part of the BP. Once all devices have acquired a unique BS, the contraction phase (CP) can start to minimize the BPL, finally data can be sent either by reserving collision free resources (Distributed Reservation Protocol - DRP) in the DTP or through prioritized contention access (PCA) [3], similarly to the enhanced distributed contention access (EDCA) defined by the IEEE 802.11e.

3. MODELING OF THE DISTRIBUTED BEACONING

To join a network a newcomer device has to follow the standard defined mechanism of extension and contraction. This work concentrates on the study of the EP. In fact, the CP follows a simpler mechanism given that no collisions happen. The analytical model developed to evaluate the energy consumption of the EP is done for one single-hop UWB subnetwork. Time is measured in number of SF, assuming that the EP starts at SF $j = 1$. All the newcomer devices k must join an existing network, where the BPST is issued by the intermediate sink (Fig. 2). We also assume a worst case in which all the k newcomer devices start to make the access at the same SF until they have allocated their beacon frames in a unique BS. We model the EP through a two-dimensional (2-D) random walk model with parameters being the variation of the HOBS position ($\overline{\Delta H}$) and the number of SF for the allocation completion $M_{set-up}(n,k)$ (network set-up delay). We suppose that the 2-D random walk can evolve with non unitary step. Parameter n indicates the EW.

The network set-up delay $M_{set-up}(n,k)$ is a random variable describing the time until absorption for a Markov chain (MC) having one absorbing state and all the others transient (Fig. 3), where $i \leq k\ \forall k \leq n$; $i = n-1\ \forall k > n$ and $i \neq k-1\ \forall k$. The absorbing state ($k-i=0$) is reached when the allocation ends and we assume a closed system in which no additional newcomer devices enter the system until the current k are allocated. According to our model, the time between two consecutive allocations follows a geometrical distribution. Relying on the analysis developed in [8], we examine two relevant cases separately: $k \leq n$ and $k > n$.

The canonical form of the transition matrix $\mathbf{P}$ of an absorbing MC is

$$\mathbf{P} = \begin{bmatrix} \mathbf{Q} & \mathbf{R} \\ \mathbf{0} & \mathbf{I} \end{bmatrix}$$

where $\mathbf{I}$ is an r-by-r identity matrix, $\mathbf{0}$ is an r-by-t matrix, $\mathbf{R}$ is a non-zero t-by-r matrix of transitions towards the absorbing state, and $\mathbf{Q}$ is the t-by-t matrix of transitions among the transient states [5]. The first t states are transient and the last r states are absorbing. For our purpose $r = 1$ and the elements $q_{h,i}$ are defined as: $q_{h,i} = Pr\{s(j) = i|h\}$. This is the probability to be in the state i of the absorbing MC at the j-th SF, $s(j) = i$, given that the process starts from the state h, where $2 \leq h \leq k$ is the current state of the MC model and $1 \leq i < k$ is the arrival state. The fundamental matrix is defined as $\mathbf{M} = (\mathbf{I} - \mathbf{Q})^{-1}$. The entry $m_{h,i}$ of $\mathbf{M}$ gives the expected number of SF to arrive in the transient state i given that the process starts in the (transient) state h. Besides, we indicate with $M_h(n,k)$ the aggregated time (in number of SF) required to reach the h-th state given that the process of allocation begins at the k-th state (the initial value of the population) and that EW is of n slots. It is therefore $M_{set-up}(n,k) = M_{k-i}(n,k)$ with $h = k-i$ the absorbing state (Fig. 3). For evaluating $M_h(n,k)$ two additional SF are needed to acquire the BS and achieve the consensus. We define the BPL at the j-th SF as:

$$BPL(j)=HOBS(j)+min\{n,mMaxBPLength-HOBS(j)\}+1 \quad (1)$$

where $HOBS(j) = HOBS(j-l) + \overline{\Delta H}(j)$, for all $j > l$ and *HOBS(0)* is the position of the HOBS before the EP starts. For a given k, the BPL is a function of the discrete times $M_h(n,k)$.

Let us now indicate with z the position of the HOBS inside n, with c, $c = [0, 2, ..., k]$ the number of devices under collision, with $s = k - c$ the number of devices successfully registered in the BP, and with ν, $1 \leq \nu \leq \lfloor \frac{c}{2} \rfloor$ the possible number of slots in collision, being $\lfloor \frac{c}{2} \rfloor$ the maximum integer number of pairs. Finally, for any value of h the total number of ways to allocate h devices into n slots is given by n^h.

The analysis focuses now on the computation of the elements $q_{h,i}$ of the matrix $\mathbf{Q}$ for the two mentioned cases $k \leq n$ and $k > n$. In both cases, we first calculate the probability $p_h(c,z)$ to choose the slot z as the HOBS (amongst n) for all the possible configurations of collision for the c devices out of the h requesting. Beside, the pair (h,i) identifies the number of devices under collision.

1) The case for $k \leq n$

When $c = 0$ (no collisions)

$$p_h(0,z) = h!\frac{1}{n^h}\binom{z-1}{h-1}, \text{ and } q_{h,0} = \sum_{z=1}^{n} p_h(0,z). \quad (2)$$

When the number of colliding devices is instead $c \geq 2$, ν slots might be under collision. Since z is the HOBS, we need to choose other $\nu + k - c - 1$ occupied slots from the remaining $z-1$. In this case, the probability $p_h(c,z)$ is modified as:

$$p_h(c,z) = \frac{h!}{c!}\frac{1}{n^h}\sum_{\nu=1}^{\nu_{max}}\binom{z-1}{\nu+h-c-1}\binom{\nu+h-c}{h-c}V(\nu,c) \quad (3)$$

where $\nu_{max} = \lfloor \frac{c}{2} \rfloor$ and $V(\nu,c)$ is the number of possible collisions configuration of c devices in ν slots. $V(\nu,c)$ is calculated using the exponential generating functions and the binomial theorem. Proof is omitted here due to space constraints. Analogously to the case $c = 0$, the probabilities $q_{h,i}$ are calculated summing over the variable z (see (2)).

2) The case for $k > n$

We compute the probabilities $q_{h,i}$ as a function of the number of successes $s = k - c$ rather than the number of colliding devices. In fact, until $k > n$ a maximum of $(n-1)$ devices can be successfully allocated. As in the previous case, we first calculate the probabilities $p_h(c,z)$ using equation (3) with $\nu_{max} = s$, and then we compute the probabilities $q_{h,i}$.

3) Energy consumption and network set-up delay computation

The expected variation of the HOBS position $\overline{\Delta H}(j)$ can be calculated as follows:

$$\overline{\Delta H}(j) = \sum\nolimits_{z=1}^{n} z \sum\nolimits_{c\neq 1}^{k} p_h(c,z). \quad (4)$$

where it is assumed that h devices (state h) are remaining at superframe j. The way $\overline{\Delta H}(j)$ is defined plays an important role in the choice of the BS. In fact, $\overline{\Delta H}(j)$ tends to be rapidly equal to the greatest size of n. An explanation to this behavior is given by the n-th order statistics. The energy consumption at the j-th SF, $E(j)$, for any device is modeled as:

$$E(j) = (BPL(j) - 1) \times E_{rx} + E_{tx}. \quad (5)$$

where the values of the energy spent in transmission (TX) and in reception (RX) are $E_{TX} = (V * I_{TX}) * L_{BF}/R_b$ and $E_{RX} = (V * I_{RX}) * L_{BF}/R_b$, respectively. L_{BF} is the length of the beacon frame (in bits) and R_b is the BP transmission rate. It is possible to upper bound the actual L_{BF} with the length of a BS. The total energy consumption $E_{tot}(n,k)$ is given by the following formula:

$$E_{tot}(n,k) = \sum_{j=0}^{M_{set-up}(n,k)} E(j) \times I_h(n,h) \times \delta(j - I_h). \quad (6)$$

where $I_h = \sum_{i=k-h+2}^{k} m_{h,i}(n,k)$, $2 \leq h \leq k$; $\delta(j - I_h)$ is the Dirac function while $E(j)$ is computed according to (5).

Table 1: Numerical values used during EP analysis

Parameter	Symbol	Value
SF duration	T_{SF}	$65.336\mu s$
BS duration	$mBeaconSlotLength$	$85\mu s$
EW	n	$1 \div 8$
Maximum BP length	$mMaxBPLength$	96 slots
BP rate	R	$53Mbps$
Operating voltage	V	$3.6V$
Current absorption in TX	I_{TX}	$200mA$
Current absorption in RX	I_{RX}	$350mA$
Power consumption in TX	P_{TX}	$720mW$
Power consumption in RX	P_{RX}	$1260mW$
Commercial battery capacity	C_b	$1200mAh$

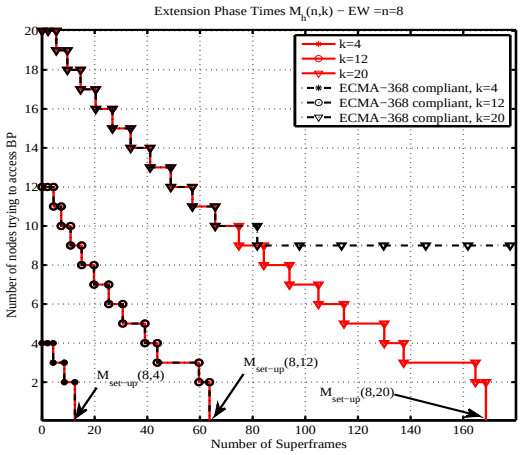

Figure 4: Times $M_h(8;k)$ in number of SF and network set-up delay times $M_{set-up}(8;k)$. for fixed $EW = n = 8$ and different values of devices population k. Standard compliant ECMA-368 includes mMaxBPLength control.

The absorbing process does not evolve with unite step size, therefore the index h is updated to $h = h + 1$ only when $j \geq I_h$.

4. RESULTS

Numerical values used for the evaluation of the energy consumption are listed in Table 1.

The times $M_h(n,k)$ are computed by solving the MC model of Fig. 3, for different values of the initial population of devices $k = \{4, 12, 20\}$ and plotted in Fig. 4. Curves in Fig. 4 show the theoretical average converging time for the EP (or the absorbing time of the MC model). We compare the curves obtained for the case of an unbounded BPL (curves non ECMA-368 compliant) with the ECMA-368 compliant case. For a population of devices $k = 4$ and $k = 12$ we obtain overlapping curves. Instead, for $k = 20$ we have two different configurations of convergence. In fact, in the standard compliant case a deadlock happens because BPL=mMaxBPLength before all the 20 devices join the BP. Correspondingly, Fig. 5 shows the length of the BP (calculated as in (1)) for $k = \{4, 12, 20\}$ and for both the above cases. Fig. 4 shows that when k is high, also the number of collisions is high but the probability that "at least one device acquires a unique BS" is higher than in the case of

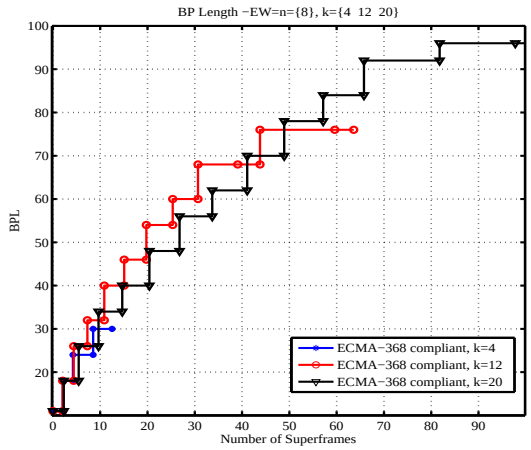

Figure 5: BPL evolution for $EW = n = 8$ slots and different values of devices population k.

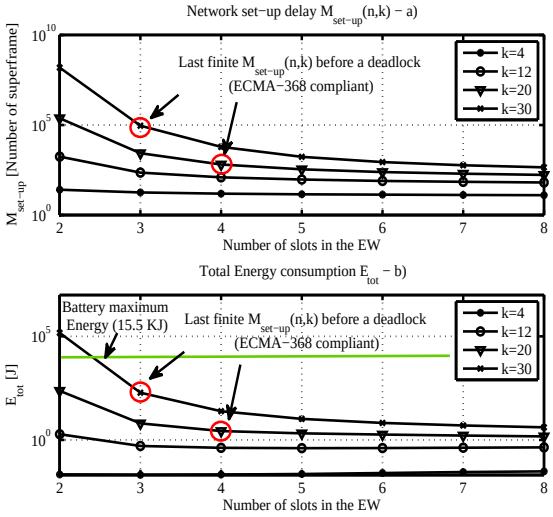

Figure 6: a) Network set-up delay; b) Total energy consumption E_{tot} for different size of the $EW(n = \{2, .., 8\})$ and different values of devices population k.

smaller k. Figure 6 shows the allocation completion times $M_{set-up}(n, k)$ and the total energy consumption $E_{tot}(n, k)$ curves, for different values of n and k. For a value of k, it exists a value of n for which all the k devices can join the BP without suffering of a deadlock. For $k = \{20, 30\}$ the deadlock is avoided respectively with $n = 3$ and $n = 4$ (the BPL is ECMA-368 compliant and $M_{set-up}(n, k)$ is a finite value). For $k = 20$, we can note that $E_{tot}(2, 20) = 230J$ and the percentage of the energy consumed during EP is approximately 1.5% of the total energy of a commercial battery. The case with $k = 30$ is not feasible for EW size $n = 2$ slots because the battery is drained before the allocation completion.

Assuming to deploy 500 geophones over a grid area $A_{max} = 500 \times 100\ m^2$ (with spatial density of $\lambda_s = 500/A_{\max} = 0.01$ nodes/m^2) where each sensor has a radio range $r = 30m$, the number of newcomer devices joining the network can be up to $k = \lambda_s \pi r^2 \simeq 30$. From Fig. 6, we can conclude that $k = 30$ requires an EW of $n = 3$ slots while the total energy consumption of the EP is $E_{tot} = 190J$ (i.e. 1.2% of the total energy of a commercial battery).

5. CONCLUSIONS

Distributed and synchronized MAC architecture is considered an attractive solution for WSN used for seismic monitoring and sub-surface diagnostic. This paper proposes the standard ECMA-368 to be applied for WSNs supporting the MB-UWB physical layer and evaluates a distributed beaconing procedure. We developed a closed form expression for the HOBS increment as a function of number of superframes. Consequently, we model the changes of the length of the beacon period and calculate the overall energy consumption associated only with the extension phase of the distributed beaconing, purposely not addressing the contraction phase. In fact, collisions cannot happen during it.

It is interesting to notice that all the investigated metrics are only a function of the extension window size n and the initial device population k. The results show that as k increases and n is set to its maximum value the HOBS has the tendency of causing an early saturation of the BP, determining a deadlock if it happens before all devices have been allocated. Therefore, we compared the standard compliant beaconing with the non standard one (no limitation to the length of the beacon period). Results of the energy consumption show that for high values of k and n, the allocation process drains entirely the battery before allocation completion. A high k finds an easy justification given the particular type of sensor network applications under consideration. Size of the EW avoiding this situation has been found to be $n = \{3, 4\}$ slots.

6. REFERENCES

[1] A. Batra and J. Balakrishnan. Design of a multiband ofdm system for realistic uwb channel environments. *IEEE Trans. on Micro. Theory and Tech.*, 52(9):2123–2137, September 2004.

[2] EC. Decision of 21/ii/2007 on allowing the use of the radio spectrum for equipment using ultra-wideband technology in a harmonised manner in the community.

[3] ECMA-368. High rate ultra wideband phy and mac standard.

[4] FCC. Revision of part 15 of the commission'srules regarding ultra-wideband transmission systems. *First Report and Order FCC 02-48.*

[5] R. Nelson. *Probability, stochastic processes, and queueing theory.* Proc. The Mathematics of Computer Performance Modeling, Springer, New York, 2000.

[6] S. Roy and al. Ultra-wideband radio design: the promise of high speed, short-range wireless connectivity. *Proc. of the IEEE.*

[7] S. Savazzi and U. Spagnolini. Wireless geophone networks for high density land acquisitions: technologies and future potential. *Special Section: Seismic Acquisition, The Leading Edge.*

[8] V. M. Vishnevsky and al. Study of beaconing in multihop wireless pan with distributed control. *IIEEE Trans. on Mobile Computing*, 7(1):113–126, January 2008.